CAPTURE OF FREE-FLYING PAYLOADS WITH FLEXIBLE SPACE MANIPULATORS

T.Komatsu, M.Uenohara, S.Iikura
R&D Center, Toshiba Corporation
Kawasaki, Japan

H.Miura, I.Shimoyama
The University of Tokyo
Tokyo, Japan

Abstract

The purpose of this paper is to discuss a recently developed control system for capturing free-flying payloads with flexible manipulators. Three essential points in this control system are, calculating optimal path, using a vision sensor for an external sensor, and active vibration control. Experimental results are shown using a planar flexible manipulator.

1. Introduction

In the near future, capture of free-flying payloads, for example, recovery of satellites, will become one of the most important tasks for manipulators on the space station. This task of space manipulators are different from those on the earth. Manipulators have to capture payloads without impact. Most space manipulators should be structurally flexible, reflecting the necessity for their light-weight based upon minimum energy comsumption and shipping cost, as well as handling of large mass payloads in a no gravity environment. Therefore, it is also necessary to control structural vibration in these space manipulators to accomplish this task, especially after capturing satellites. The purpose of this paper is to discuss a recently developed control system for capturing free-flying payloads with flexible manipulators. Experimental results are shown using a planar flexible manipulator.

Three essential points in this control system are, (1)calculating optimal path of manipulator tip, (2)direct sensing of position and attitude of a payload using a hand eye camera, and (3)active vibration control of a manipulator. Determining the optimal path is necessary to accomplish non impact capture of a payload. This path is obtained by minimizing the performance index which consists of relative position error, velocity error and acceleration of manipulator tip. Direct sensing of the relative position between a manipulator and a payload is necessary to move the manipulator tip precisely along the optimal path. The authors used a hand eye CCD camera and LED target marker for this sensor. Active vibration control is necessary for precise and quick control of a manipulator. A local PD feedback of joint angle and torque was used for robust positioning and vibration control.

An experimental equipment was built to investigate the validity of this control system. This equipment consists of an air suspended, flexible two-link manipulator, a payload, and a controller. Experimental results of capturing a moving payload demonstrates the effectiveness of this system.

2. Control System

The task of a manipulator considered in this paper is automatic capture

of free-flying payloads, for example, capture of satellites, with manipulators on the space station or on the free-flyer. This task was accomplished in the Space Shuttle program by cooperation between RMS (remote manipulator system) and EVA (extra vehicular activities). This task was done for repair of a disabled satellite. In the future, after constructing the space station, many satellites will be assembled on the station and thrown into an orbit. Therefore, maintenance and repair of satellites will be done frequently on an orbit. In such a case, doing this task manually will be expensive and uneffective. Therefore accomplishing this task automatically is necessary.

To construct control system for the first stage, the following assumptions were made for payload motion.

(1)A payload rests or moves with constant velocity to the manipulator's base.
(2)A payload does not revolve on its own axis.
(3)Movement of a payload is constrained on one plane.

For using this control system on an orbit, the following capabilities are targeted:

(a)Real time manipulator path planning
(b)Direct sensing of the payload position
(c)Quick and precise motion control of a manipulator
(d)Easy integration

The system can be represented by Figure 1. The major subsystems are:

(1)Path planning
(2)Vision system
(3)Manipulator control

Explanation of the subsystem is as follows:

2.1 Path planning

In this subsystem, an approach path of a manipulator is calculated in real time. The following assumptions were made:
(1)A free-flying payload moves straight with constant velocity.
(2)The position and velocity of calculated path become equal to those of free-flying payload at the target time t_f.

The authors chose the optimal path obtained by minimizing the following performance index as the approach path satisfying upper assumptions.

$$J=\frac{1}{2}(\boldsymbol{X}^t S_f \boldsymbol{X})_{t_f}+\frac{1}{2}\int_{t0}^{tf} \boldsymbol{a}_m{}^t \boldsymbol{a}_m dt \qquad (1)$$

where

$$\boldsymbol{\kappa}=\boldsymbol{\kappa}_p-\boldsymbol{\kappa}_m$$

$\boldsymbol{\kappa}_p$: The position vector of a free-flying payload
$\boldsymbol{\kappa}_m$: The position vector of a manipulator path

$$\boldsymbol{X}=\begin{bmatrix}\dot{\boldsymbol{\kappa}}\\ \boldsymbol{\kappa}\end{bmatrix}=(Vx,\ Vy,\ Vz,\ X,\ Y,\ Z)^{t}$$

$$S_f=diag(C_1,\ C_1,\ C_1,\ C_2,\ C_2,\ C_2)\qquad (C_1,\ C_2\to\infty)$$

$$\boldsymbol{a}_m=\ddot{\boldsymbol{\kappa}}_m$$

By using this path, non impact capture is realized because position error and velocity error between a manipulator and a payload become zero at t_f. Moreover, smooth path is obtained because of minimizing total sum of $(\boldsymbol{a}_m)^2$.

Considering $\boldsymbol{a}_m$ as the input to the system, the following system equation is obtained because the acceleration of a payload is zero.

$$\dot{\boldsymbol{X}}=F\cdot\boldsymbol{X}+G\cdot\boldsymbol{a}_m \tag{2}$$

where

$$F=\left[\begin{array}{ccc|c} & & & \\ & 0 & & 0 \\ & & & \\ \hline 1 & 0 & 0 & \\ 0 & 1 & 0 & 0 \\ 0 & 0 & 1 & \end{array}\right]\qquad G=\left[\begin{array}{ccc} -1 & 0 & 0 \\ 0 & -1 & 0 \\ 0 & 0 & -1 \\ \hline & & \\ & 0 & \\ & & \end{array}\right]$$

Therefore, solving optimal path from equation (1) is equal to the design of the linear inhomogeneous regulator. In general, for this problem, the system equation, the cost function and its general solution become as follows [1]:

$$\dot{\boldsymbol{y}}=F(t)\,\boldsymbol{y}+G(t)\,\boldsymbol{u}+C(t) \tag{3}$$

$$J=\frac{1}{2}(\boldsymbol{y}^{t}S_f\boldsymbol{y})_{tf}+\frac{1}{2}\int_{t0}^{tf}(\boldsymbol{y}^{t}A\boldsymbol{y}+\boldsymbol{u}^{t}B\boldsymbol{u})\,dt \tag{4}$$

$$\boldsymbol{u}(t)=-B^{-1}G^{t}S\boldsymbol{y}-B^{-1}G^{t}K \tag{5}$$

$$\dot{S}=-SF-F^{t}S+SGB^{-1}G^{t}S-A \tag{6}$$

$$S_f=S(tf)$$

$$\dot{K}+(F^{t}-SGB^{-1}G^{t})K+SC=0 \tag{7}$$

$$K(tf)=0$$

Compairing equation (1) and (2) with (3) and (4),F and G equal equation (2), and $\boldsymbol{y},\boldsymbol{u},B,A,C$ become as follows:

$$\boldsymbol{y}=\boldsymbol{X}\qquad\qquad \boldsymbol{u}=\boldsymbol{a}_m \tag{8}$$

$$B=\begin{bmatrix}1&0&0\\0&1&0\\0&0&1\end{bmatrix} \qquad A=C=0.$$

Substituting these equations into equation (5)$\sim$(7), the analytical solution is obtained as follows:

$$\begin{bmatrix}a_{mX}\\a_{mY}\\a_{mz}\end{bmatrix}=\begin{bmatrix}\dfrac{4}{(tf-t)}V_X+\dfrac{6}{(tf-t)^2}X\\\dfrac{4}{(tf-t)}V_Y+\dfrac{6}{(tf-t)^2}Y\\\dfrac{4}{(tf-t)}V_Z+\dfrac{6}{(tf-t)^2}Z\end{bmatrix} \tag{9}$$

The optimal path is calculated by the integral of equation (9) substituting V_x, V_y, V_z, X, Y, Z which are obtained from vision system in real time.

2.2 Vision system

In this system, position and attitude data of a payload are sensed in real time. This system consists of a CCD camera, a marker and an image processing unit. A CCD camera watches a target marker on a payload. This marker consists of a rectangle formed by 4 LED points. Next, video signal from a CCD camera is sent to image processing unit. In this unit, coordinates of 4 LED points in the frame are detected using a simple hardware.

In three dimensional space, when the geometric relation of 4 points on a plane are known and corresponding points to 4 points are obtained in the frame, three dimensional coordinates of these points are determined by using inverse translation of projection. Therefore, three dimensional coordinates of a payload can be detected only by a monocular camera. Figure 2 shows coordinates of a camera$_f$(Σ C) which consist of X^c, Y^c and Z^c, and a frame which consist of X^f, Y^f. For each 4 LED points, the following equations are obtained from translation of projection.

$$\begin{bmatrix}X_i^c\\Y_i^c\\Z_i^c\end{bmatrix}=k_i\begin{bmatrix}X_i^f\\y_a\\Y_i^f\end{bmatrix} \qquad (i=1,\cdots,4) \tag{10}$$

where

$$k_1=\sqrt{\frac{L_{13}^2}{(X_1^f-k'_3\ X_3^f)^2+(Y_1^f-k'_3\ Y_3^f)^2+(1-k'_3\ )^2 y_a^2}} \tag{11}$$

$$\begin{bmatrix} k'_2 \\ k'_3 \\ k'_4 \end{bmatrix} = \begin{bmatrix} X_2{}^f & -X_3{}^f & X_4{}^f \\ y_a & -y_a & y_a \\ Y_2{}^f & -Y_3{}^f & Y_4{}^f \end{bmatrix}^{-1} \begin{bmatrix} X_1{}^f \\ y_a \\ Y_1{}^f \end{bmatrix} \qquad k_i = k_1 k'_i \qquad (i=2, 3, 4)$$

and

$$\phi = \tan^{-1}\left(\frac{X_1{}^c - X_4{}^c}{Z_1{}^c - Z_4{}^c}\right) \qquad \theta = \cos^{-1}\left(\frac{Z_1{}^c - Z_4{}^c}{L_{14}\cos\phi}\right) \qquad (12)$$

$$\psi = \cos^{-1}\left[\frac{1}{L_{12}}\{(X_2{}^c - X_1{}^c)\cos\phi - (Z_2{}^c - Z_1{}^c)\sin\phi\}\right]$$

ϕ, θ, ψ denote role, pitch, yaw of a marker. L_{ij} denotes the actual length between No. i and No. j. Therefore, three dimensional data X^c, Y^c, Z^c, ϕ, θ, ψ of a marker are detected by sensing X^f and Y^f. In this system, data are obtained at 50 msec intervals.

2.3 Manipulator control

Most of space robots must be structurally flexible, reflecting the necessity for their light-weight based upon minimum energy consumption and shipping cost, as well as handling large mass payloads in a no gravity environment. Therefore it is necessary to control the structural vibration in the flexible arm for quick, precise tracking of the trajectories and accomplishment of tasks.

Figure 3 shows a blockdiagram of manipulator control. The outer loop is for motion control. The inner loop is for vibration control. In this method, joint angle and torque sensors are basically needed, which are ordinarily used in remote manipulator systems for nuclear power plants.

We derived this method from the standpoint of energy control in the system, where the energy was both kinetic and potential. We considered a flexible manipulator system as a completely mechanical system. From this standpoint, it is possible to consider that the control of a flexible manipulator is the same as the control of two types of mechanical springs in a system. The first one is springs in an elastic link. These springs cause structural vibrations of all modes when the accumulated potential energy converted to kinetic energy. So it is necessary to minimize both kinetic and potential energy at the target point for vibration restraint.

The second one is a spring in an actuator. For example, if the manipulator motion is controlled by simple proportional and derivative (PD) feedback compensation, as the general industrial robots, the work accomplished by this actuator is the same as the work in a general linear spring. In this case, the proportional control gain equals the spring constant. It is also necessary to minimize both the kinetic and potential energies of this spring at the target point for motion control [2].

In the case of flexible manipulators, both vibration and motion control are needed at the same time. Therefore, it is necessary to control both springs. In this control, total energy control for the system is accomplished by composing both joint angle and torque PD feedback loops. The position feedback loop realizes grobal motion control, while the joint torque feedback loop realizes vibration control of all modes [3].

3. Experimental setup

An experimental equipment was built to investigate the validity of this system. The authors named this equipment TESRA-I (teleoperated elastic space robot arm). This equipment consists of a two dimensional air suspended flexible manipulator, a payload and a controller. Figure 4 shows configuration of this equipment.

The flexible manipulator is about 1.5 meter long. It has two flexible links and three degrees of freedom (shoulder, elbow, wrist). An actuator is installed at each joint. It consists of a DC motor and a planetary gear reducer (1:100 reducer ratio). The sensor system consists of a potentiometer for sensing the joint angle, a tachogenerator for sensing the motor velocity, and the strain gages at the joint axis for sensing the joint torque. Flexible links for this manipulator are made form strainless steel. The link diameter is 6mm. The total weight for each joint and hand are 4kg and 1kg. This arm floats on an acrylic plate base, using four air bearings so as to simulate a no gravity environment in the horizontal plane. A small CCD camera, 35mm(W) x 43mm(H) x 70mm(L), is installed on the manipulator's hand (Fig.5).

The payload consists of lead sheets, and the weight is 40kg. A handle for grasping is installed at one side of this payload and a target marker is attached on it. This marker consisted of a rectangle formed by 4LED points, 40mm(W) × 30mm(H).

This manipulator is controlled by a MOTOROLA digital computer VME-10 system as the main computer. Its MPU is the 16-bit 68010, and the VERSAdos multitasking system is used as the operating system. Sensor outputs are sampled at 15msec intervals through a 32ch A/D board. Commands are fed to the servo amplifiers through the 4ch D/A board. In the vision system, 32-bit MPU(68020) are used for calculation of the target position.

4.Experimental result

Figure 6 shows one of experimental results of capturing a free-flying payload, and the paths of manipulator tip and a payload are indicated.

The task sequence from capture to stop is as follows. The time of capture t_f is 6.0sec. The path are planned so that manipulator tip goes to the location of about 1cm from a handle for grasping a payload. And, after arriving at the location, manipulator tip goes ahead and captures a payload.

(1)A payload is manually accelerated to get to about 5cm/sec speed, and released.
(2)An optimal path is calculated, and a manipulator is controled so as to track the planned path.
(3)A manipulator tip arrives at the location of about 1cm from a handle for grasping a payload at 6.0 seconds.

(4)A manipulator tip goes ahead for grasping a handle.
(5)Capturing of a payload finishes at 10 seconds.
(6)A manipulator stops a payload at 30 seconds.

It is obvious that a manipulator tip moved along a smooth path and captured a payload without impact. A little impact shown in figure 6 was caused when two fingers of a manipulator closed. No link vibration occured after stopping the payload.

5. Conclusions

In this study, the authors proposed a recently developed control system for use in automatic capturing free-flying payloads with a flexible manipulator. The features of this system are as follows:

(1)real time path planning
(2)direct sesing of payload position by a vision system
(3)quick and precise control of a flexible manipulator
(4)easy integration.

The effectiveness of this system has been verified by experimental results. The next step for this sytem is to expand its ability so as to adapt it to capture a payload with acceleration and revolution on its own axis, and finally adapt it to real three dimensional system.

References

1. V.Carber: Optimal Intercept Laws for Accelerating Targets, AIAA Journal, No.6, Vol.11, 6-11, (1968)

2. M.Takegaki and S. Arimoto: A New Feedback Method for Dynamic Control of Manipulators, ASME Journal of Dynamic Systems, Measurement, and Control, Vol. 102, 119-125, (1981)

3. T.Komatsu, M.Uenohara, S.Iikura, H.Miura and I.Shimoyama: Active Vibration Control for Flexible Space Environment Use Manipulator, IFAC, Zurich, Switzerland (1988)

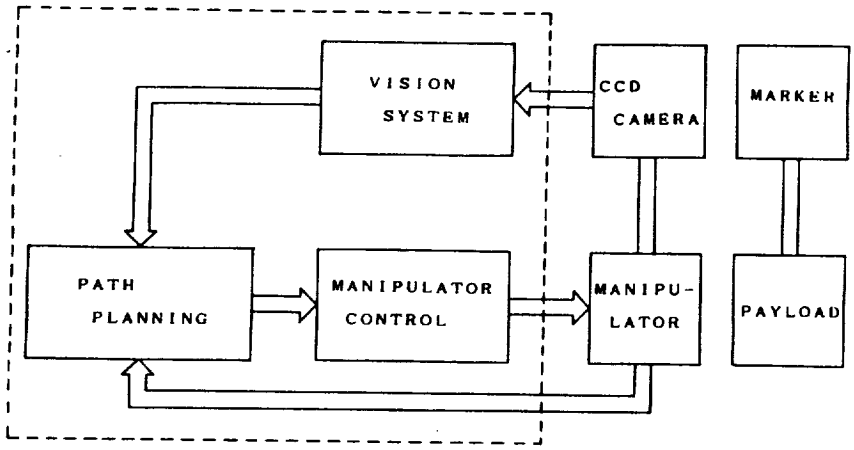

Fig. 1 Control System Architecture

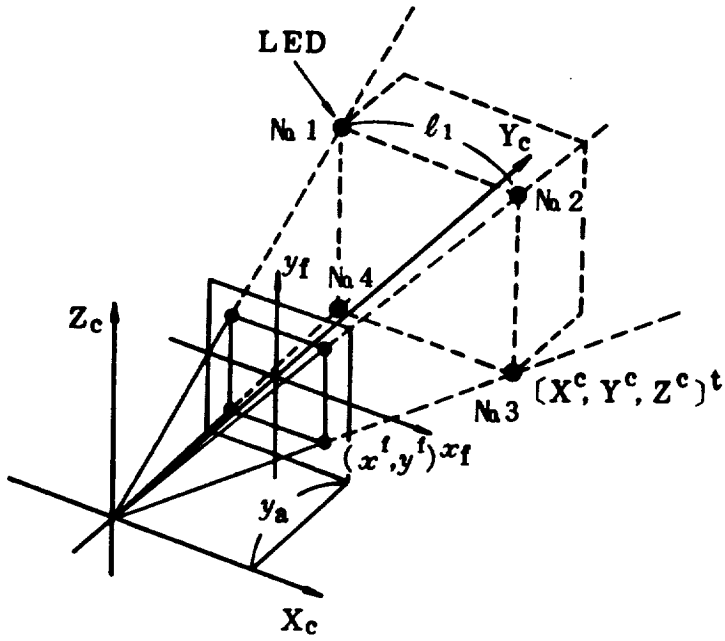

Fig. 2 Translation of Projection

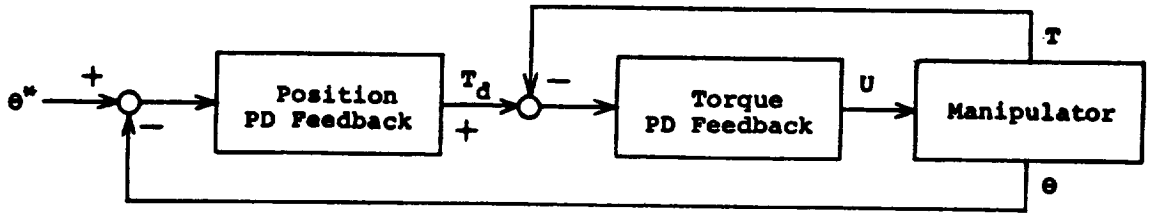

Fig. 3 Block diagram of Manipulator Control

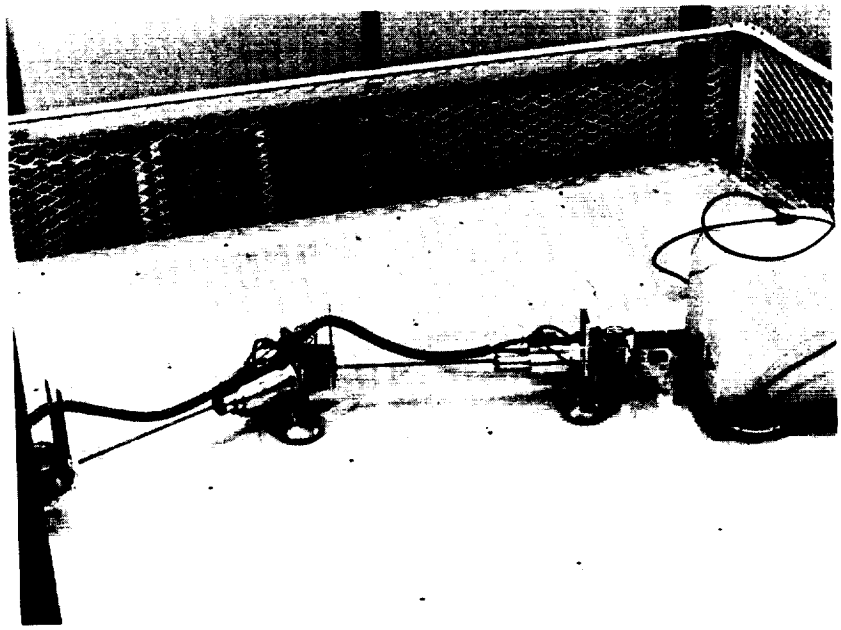

Fig. 4 TESRA I Configuration

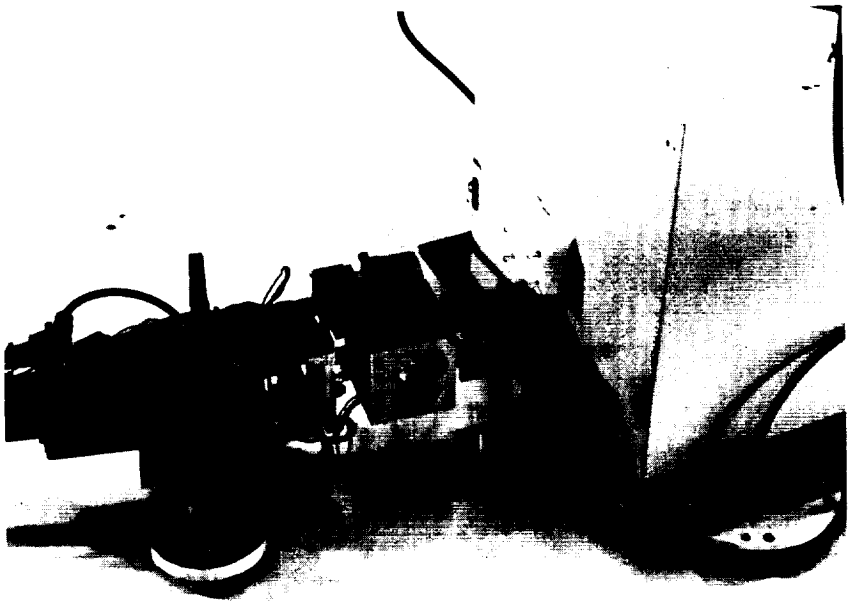

Fig. 5 CCD Camera and Target Marker

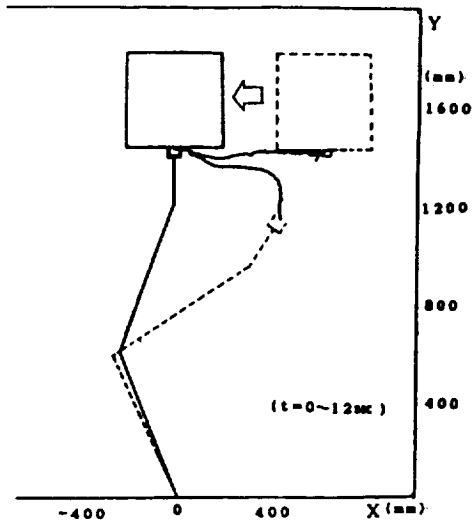

(a) Tracking Path in the XY Plane

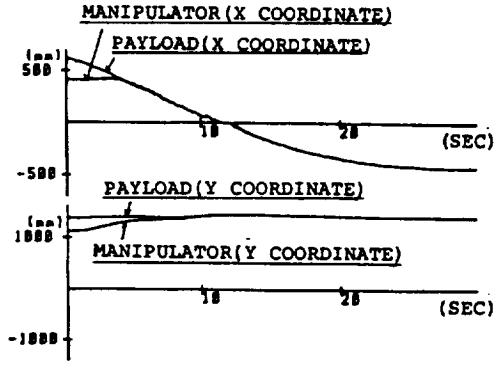

(b) Position of a Manipulator and a Payload

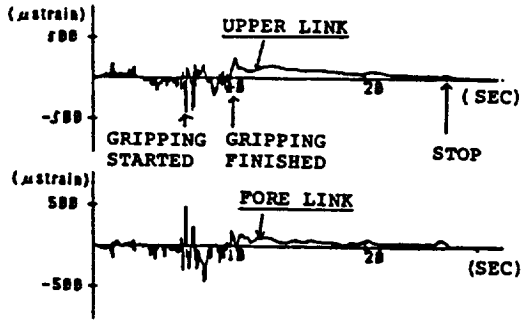

(c) Link Vibration

Fig. 6 Experimental Results